

**Title:**

A Polarization-Independent Liquid Crystal Spatial-Light-Modulator

**Authors:**

Michael J. Escuti and W. Michael Jones

**Affiliation:**

North Carolina State University, Dept Electrical & Computer Engineering, Raleigh, NC (USA)

**Presented At:**

*SPIE Optics & Photonics Conference*, San Diego, CA (August 13-17, 2006)

**Citation:**

M.J. Escuti and W.M. Jones, "A Polarization-Independent Liquid Crystal Spatial-Light-Modulator", *Proceedings of SPIE*, vol. **6332**, no. 63320M (2006).

Copyright 2006 Society of Photo-Optical Instrumentation Engineers.

This paper was published in Proceedings of SPIE Vol. 6332 and is made available as an electronic reprint with permission of SPIE. One print or electronic copy may be made for personal use only. Systematic or multiple reproduction, distribution to multiple locations via electronic or other means, duplication of any material in this paper for a fee or for commercial purposes, or modification of the content of this paper are prohibited.

# A Polarization-Independent Liquid Crystal Spatial Light Modulator

Michael J. Escuti and W. Michael Jones

North Carolina State Univ, Dept Electrical & Computer Engineering, Raleigh, NC (USA)

## ABSTRACT

We report our recent experimental results on a new polarization-independent, liquid crystal (LC) spatial light modulator (SLM). Based on a periodic nematic director profile, the modulator acts as a switchable diffraction grating with only  $0^{th}$ - and  $\pm 1^{st}$ -orders at efficiencies of  $\geq 99\%$ , manifests contrast ratios  $\sim 600:1$  (for laser light), switching times of  $\sim 2ms$ , and threshold voltages of  $< 1V/\mu m$ . Results of modulating broadband, unpolarized light from light-emitting-diodes (LEDs) indicates that contrast ratios are  $\sim 100:1$  so far. Note that incoherent scattering for visible light is very low, and that samples are typically completely defect-free over large areas. An important feature of this diffractive polarization-independent SLM compared to its predecessors is its potential to achieve much larger diffraction angles, which enables a larger aperture (and étendue). In addition to describing the fabrication and characteristics of this SLM in general, we report on our initial progress in implementing a projection display system. All of the surprising and useful results from this grating arise from its continuous nematic director, which is most properly classed as a switchable polarization grating (PG). The SLM described here offers the inherent advantages polarization-independence at the pixel-level and fairly fast switching with nematic LCs, while maintaining similar switching voltages, cell thickness, contrast ratios, and materials.

**Keywords:** projection display, spatial-light-modulator, SLM, liquid crystal display, polarization grating, holography, photo-alignment, unpolarized light, diffractive optical element

## 1. INTRODUCTION

We aim to develop a liquid crystal (LC) spatial-light-modulator (SLM) capable of modulating unpolarized light with high contrast. Any liquid crystal device modulating unpolarized light on a pixel-level would be immensely useful as the active element in a highly efficient projection display system. Other applications that would benefit include tunable optical filters for imaging and diffractive photonic elements that are insensitive to polarization. We are developing a liquid crystal polarization grating<sup>1</sup> (LCPG) with effectively ideal experimental properties, and seek to apply them to these applications and beyond.

Previously, several polarization-independent, binary, LC gratings with the potential for polarization independent switching were studied,<sup>2-7</sup> but were ultimately limited by small diffraction angles, scattering domain boundary lines, and random disclinations. It was recognized<sup>8-10</sup> that a continuous LC diffractive grating would have improved diffraction properties (over binary LC gratings), and that holography could be used to simplify fabrication and achieve smaller grating periods. Theoretical studies<sup>9,11,12</sup> identified compelling characteristics, including the potential to modulate unpolarized light with high contrast. Experimental results starting in 2004 were promising,<sup>8</sup> but were plagued by pervasive defects crippling their optical properties due to poor LC alignment. More recent work<sup>13</sup> reported in 2006 continued to show substantial scattering due to the presence of disclinations and random defects and achieved only  $< 18\%$  efficiency .

Here we report on our *experimental realization* of a liquid crystal diffraction grating with truly ideal properties, including  $\sim 100\%$  diffraction efficiencies, high contrast (600:1), very low scattering ( $< 0.3\%$ ), low drive voltages, surprisingly fast switching, and full modulation of unpolarized LED light.

---

Correspondence should be addressed to: mjescuti@ncsu.edu, +1 919 513 7363

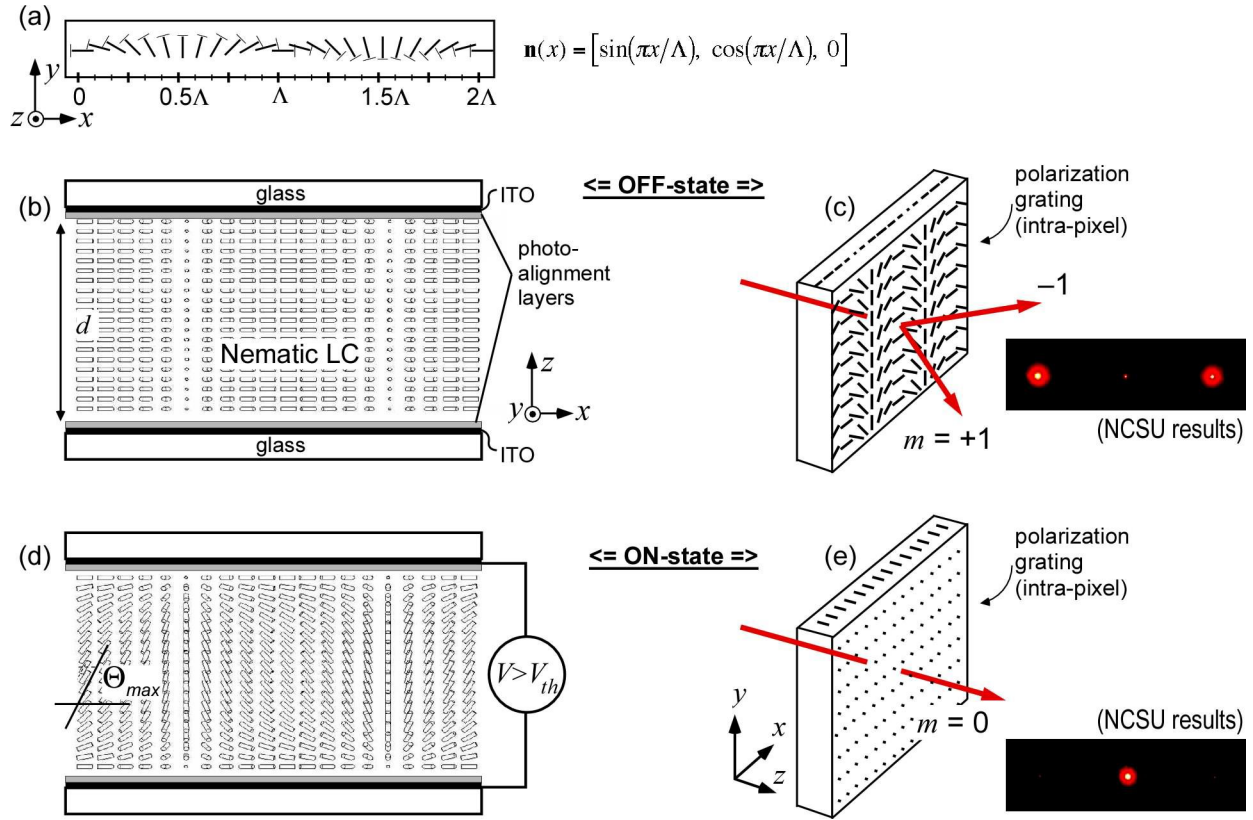


**Figure 1.** Structure and operation of the liquid crystal polarization grating (LCPG): (a) top-view and (b) side-view of continuous, in-plane nematic profile (calculated for when  $d < d_C$ ); (c) ideal diffraction when  $\Delta nd = \lambda/2$ ; (d) calculated nematic profile when applied voltage is greater than  $V_{th}$ , leading to out-of-plane reorientation and reduction of effective  $\Delta n$ ; and (e) PG is ideally erased at high applied voltages. Photographs in (c) and (e) are actual results from a PG with  $\Lambda = 6.3\mu m$ .

## 2. BACKGROUND

The little-known class of periodic structures known as polarization gratings (sometimes called anisotropic or vectorial gratings) has actually been around since the 1970s, when initial publications about the more general case of polarization holograms appeared in Soviet journals.<sup>14</sup> It was soon recognized<sup>11,12</sup> that PGs could manifest a combination of the most advantageous properties of both thick-and thin-gratings (and beyond): 100% diffraction efficiency, strong polarization sensitivity of the  $\pm 1$ -order diffraction, potential for diffraction into only first orders, and comparatively wide bandwidth.

Conventional diffraction gratings and holograms operate by periodically modulating the phase or amplitude of light propagating through them. Polarization gratings (PGs), instead operate by modulating the polarization state of light passing through, and are embodied as a spatially varying birefringence and/or dichroism. We focus here on one type in particular: an in-plane linear birefringence with optical symmetry axis that varies with position,

$$\mathbf{n}(x) = [\sin(\pi x/\Lambda), \cos(\pi x/\Lambda), 0], \quad (1)$$

which can be embodied as a liquid crystal (LC) texture as shown in Fig. 1(a) and 1(b). Note its structural similarity to the cholesteric<sup>15</sup> and fingerprint<sup>16</sup> chiral LC profiles. However, the PG structure is distinct from them because it is determined by the surface alignment, and not by chirality.

The diffraction from this elegant structure are somewhat surprising and broadly useful. Using the reasoning in Refs.<sup>1,11</sup> and assuming that  $Q = 2\pi\lambda d/n_0\Lambda^2$ , we can write the diffraction efficiencies with an explicit dependence

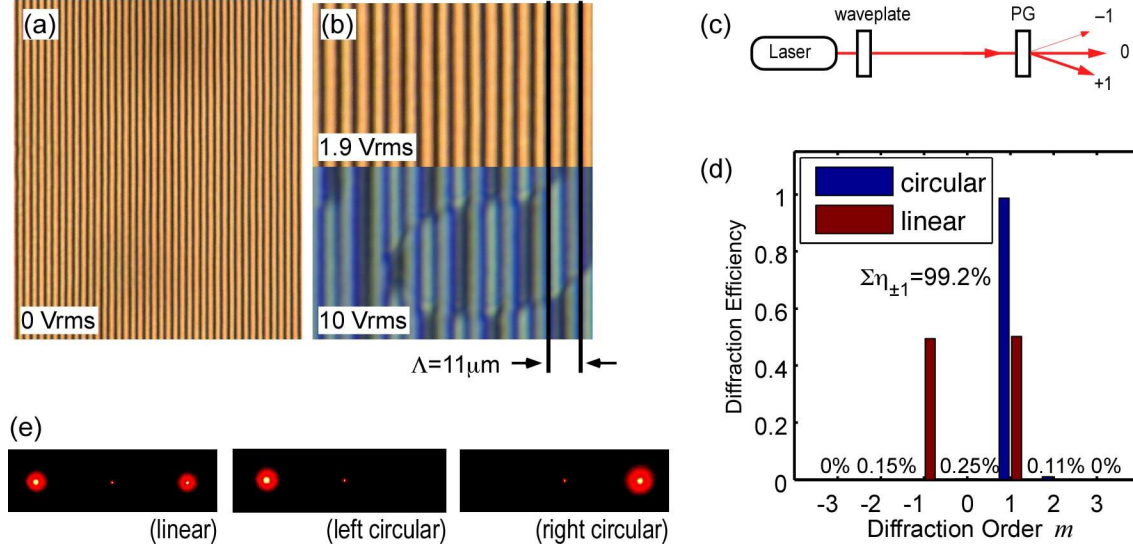


**Figure 2.** Experimental results: polarizing optical micrographs (crossed-polarizers) (a) without voltage and (b) at applied voltages higher than threshold; (c) electro-optical characterization setup for monochromatic light (HeNe, 633nm); (d) measured diffraction efficiencies and (e) photograph of diffraction for circular and linear input polarizations. ( $\Lambda = 11 \mu\text{m}$  and  $d = 2 \mu\text{m}$ )

on the polarization state of the normally-incident light (only three diffraction orders are possible):

$$\eta_0 = \cos^2 \left( \frac{\pi \Delta n d}{\lambda} \right) \quad (2)$$

$$\eta_{\pm 1} = \frac{1}{2} [1 \mp S'_3] \sin^2 \left( \frac{\pi \Delta n d}{\lambda} \right) \quad (3)$$

where  $\eta_m$  is the diffraction efficiency of the  $m^{\text{th}}$ -order,  $\lambda$  is the vacuum wavelength of incident light,  $\Delta n$  is the linear birefringence,  $d$  is the grating thickness, and  $S'_3 = S_3/S_0$  is the normalized Stokes parameter corresponding to ellipticity of the incident light. There are several notable aspects to this PG that can be observed from Eqns. (2) and (3): first, the  $\pm 1$ -order efficiencies are highly polarization sensitive; second, maximum diffraction occurs when the local retardation is halfwave ( $\Delta n d = \lambda/2$ ); third, 100% efficient diffraction into either one of the  $\pm 1$ -orders occurs when the incident light is circularly polarized; fourth, there is no dependence of the diffraction efficiency on the period of the grating (as long as  $Q \leq 1$ ); and fifth, the  $\pm 1$ -orders will always be circularly polarized with opposite handedness while the 0th-order will maintain the incident polarization.

If the profile of Fig. 1(a) is achieved, the grating will diffract light near the half-wave retardation wavelength completely, as illustrated in Fig. 1(c). An applied voltage reduces the effective birefringence and tunes the transmission spectrum (see Fig. 1(d)). When voltages are high enough, the PG is effectively erased, and light passes directly through (Fig. 1(e)). Note that the switching behavior and transmittance equations are very similar to those of a variable LC retarder,<sup>17</sup> with the key difference that no polarizers are involved in the LCPG and its maximum transmittance is therefore at least twice as large.

### 3. FABRICATION

The most significant advance in our work is that we have succeeded in experimentally realizing the LCPG structure with very good fidelity. The basic fabrication process<sup>8, 18</sup> is the same for all researchers and in our case starts with two coherent beams from an ultraviolet laser (HeCd, 325nm, dose =  $\sim 300 \text{mJ/cm}^2$ ) with orthogonal circular polarizations that are superimposed with a small angle between them, leading to an interference pattern

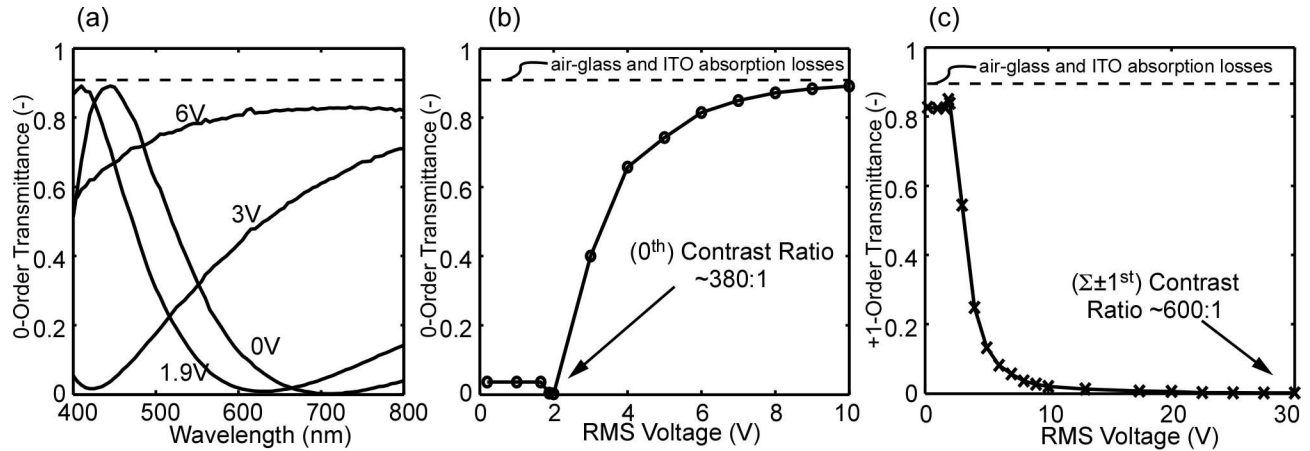


**Figure 3.** Electro-optical response of the LCPG: (a) transmission spectra revealing voltage-tuning of effect; transmittance of a HeNe laser ( $633nm$ ) for (b) the 0-order and (c) the  $\sum$  of  $\pm 1$ -orders. The results of (b) and (c) do not measurably change depending on input polarization.

with constant intensity and a periodically varying linear polarization state that follows Fig. 1(a) (with period  $\Lambda = \lambda_R/2 \sin \theta$ , where  $\lambda_R$  is the recording wavelength and  $\theta$  is the half the angle between the beams). Next, two glass substrates with indium-tin-oxide (ITO) electrodes are coated with a photo-alignment material<sup>19</sup> (ROP201, Rolic), and laminated together such that a uniform thickness ( $d = 2\mu m$  here) is maintained by an edge-seal of glue. This is then exposed by the polarization hologram capturing the pattern in the photo-alignment layers. Finally, a nematic LC (MLC-6080, Merck,  $\Delta n = 0.202$ ,  $T_{NI} = 95^\circ C$ ) fills the gap by capillary action (at  $115^\circ C$ ), and the desired LCPG structure is realized as the surfaces direct the LC orientation (Fig. 1(b)). For the results here,  $\Lambda = 11\mu m$ .

Previous experimental work with LCPGs<sup>13,18</sup> led to less-than ideal LC alignment rife with defects. We have overcome this through two primary avenues: designing cell geometry in view of the critical thickness,<sup>9,20</sup> and by extensive materials optimization (of both the LC and photo-alignment layers).

#### 4. MODULATING MONOCHROMATIC LIGHT

Micrographs of a typical sample are shown in Fig. 2(a) and (b), revealing a smoothly varying texture with no LC defects over very large areas (up to several  $cm^2$  achieved). It is this feature that enables us to achieve excellent agreement in experimental results and the predictions of Eqns. (2) and (3). Laser ( $633nm$ ) diffraction was measured in the setup shown in Fig. 2(c), and revealed almost complete diffraction within the 0- and  $\pm 1$ -orders (Fig. 2(d)) regardless of input polarization, and very little incoherent scattering ( $<0.3\%$  for red light) was routinely observed. As theoretically anticipated, the first-order intensity is strongly polarization-sensitive, and maximum diffraction efficiency of 99.2% with very high contrast (Fig. 2(e)) occurs when the input light has circular polarization.

Note that the transmittance of the LCPG is defined as  $T = I_{mod}/I_{in}$ , where  $I_{mod}$  is the modulated (output) intensity and  $I_{in}$  is the input intensity. This measure includes the effect of the cell reflections and any absorption. A slightly different measure, the experimental diffraction efficiency of the PG, is defined as  $\eta_m = I_m/(\dots + I_{-1} + I_0 + I_{+1} + \dots)$ , where the effect of the hologram is isolated, and any Fresnel (air-glass) reflection losses and ITO absorption are normalized out. All electro-optic measurements were done with a 4 kHz square wave.

Basic switching behavior is shown in Fig. 3. The voltage threshold is  $V_{th} = 1.65V$ , a value relatively close to predictions,<sup>20</sup> and comparable to conventional LC configurations.<sup>21</sup> The 0-order transmittance spectra for several applied voltages is shown in Fig. 3(a), clearly showing the tunable filter effect caused by the reduction of the birefringence. The 0- and  $\pm 1$ -order transmittance response to applied voltage is shown in Fig. 3(b) and 3(c) for monochromatic light ( $633nm$ ). The maximum 0-order contrast ratio was 380:1, and 600:1 for for the  $\pm 1$ -order

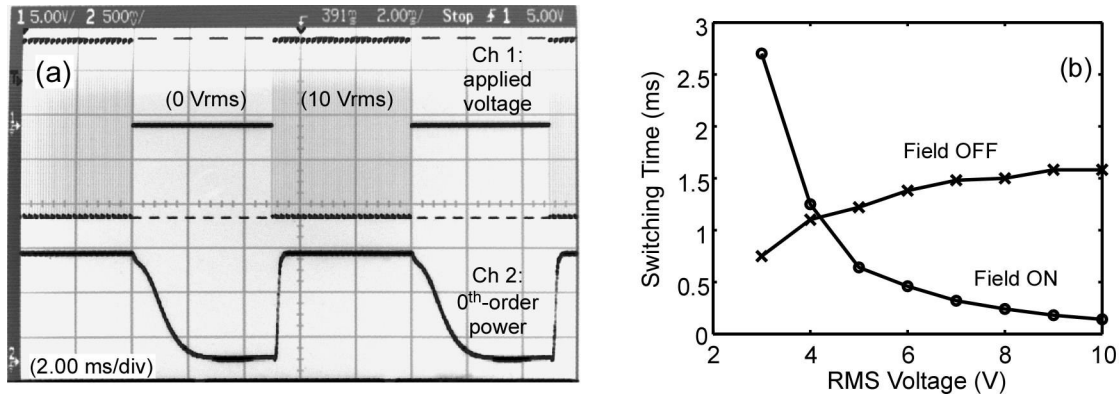


**Figure 4.** Dynamic response of the LCPG: (a) oscilloscope screenshot of drive signal and optical response; and (b) switching times as a function of applied voltage.

contrast ratio. Note that the maximum diffraction efficiency for circularly polarized light was  $>99\%$ , as can be observed in Fig. 2(d), 2(e), and 3(c).

The full-contrast switching times (10%-90% rise and fall times) are shown in Fig. 4 of the 0-order intensity were measured with the setup illustrated in Fig. 2(b). The total ON-OFF time is  $\leq 2ms$  for all voltages above 5V, which is significantly faster than previously reported<sup>18</sup> and even faster than predicted by our initial elastic free-energy analysis.<sup>20</sup> This relatively fast switching in a nematic has been verified across several samples with different grating periods and LC materials.

## 5. MODULATING UNPOLARIZED LIGHT

Multiple methods exist for image projection from a diffractive modulator, with Schlieren projection method being the most prominent.<sup>22,23</sup> Both the bright-field and dark-field Schlieren configurations are illustrated in Fig. 5. Since the LCPG only diffracts into the zero and first diffraction orders, the Schlieren system is relatively simple, with the potential to be very robust to contrast degradation due to scattering. In the bright-field configuration (Fig. 5(a)), an aperture stop is placed in such a way as to block all diffracted orders except the zero order, similar to a conventional spatial-filter. In the dark-field configuration (Fig. 5(c)), the complementary situation occurs: the zero order is blocked and the first orders are projected. The modulator achieves bright-dark contrast at any given pixel in either Schlieren configuration as it individually directs incident light into or out of the zero and first diffraction orders.

A single-pixel LCPG microdisplay element ( $\sim 2cm^2$  area) was placed in a custom-built projection system.<sup>22</sup> The light engine consisted of individual red, green, and blue LEDs (Lumileds) with several lenses for light collection from the LEDs. A single biconvex lens was used as a simple projection optic, resulting in an overall image magnification of  $\sim 15$  with a throw of 0.6 m.

The measured transmittance characteristic using the bright-field Schlieren configuration is shown in Fig. 5(b). Somewhat surprisingly, the maximum contrast ratio obtained for the red LED was 144:1 even for applied voltages 10V. Maximum bright-field contrast for the green and blue LEDs were 73:1 and 82:1. Note that the dark-state voltage is different for each color, an inherent feature of this display type. The contrast-limiting aspect of this scheme is primarily the light-leakage in the dark state due to the wide source spectral width. Unless the spectral width of the source is narrowed (e.g. with interference filters), may be difficult to improve the contrast of the bright-field projection scheme further.

The measured transmittance characteristic using the dark-field Schlieren configuration is shown in Fig. 5(d). The maximum contrast ratio obtained was 136:1 for the red LED, and lower contrasts were measured for green and blue (35:1 and 43:1, respectively). Unlike the previous case, the dark state in this mode occurs at the high voltage state, as the grating is erased. Therefore, we anticipated that the dark-field Schlieren projection scheme

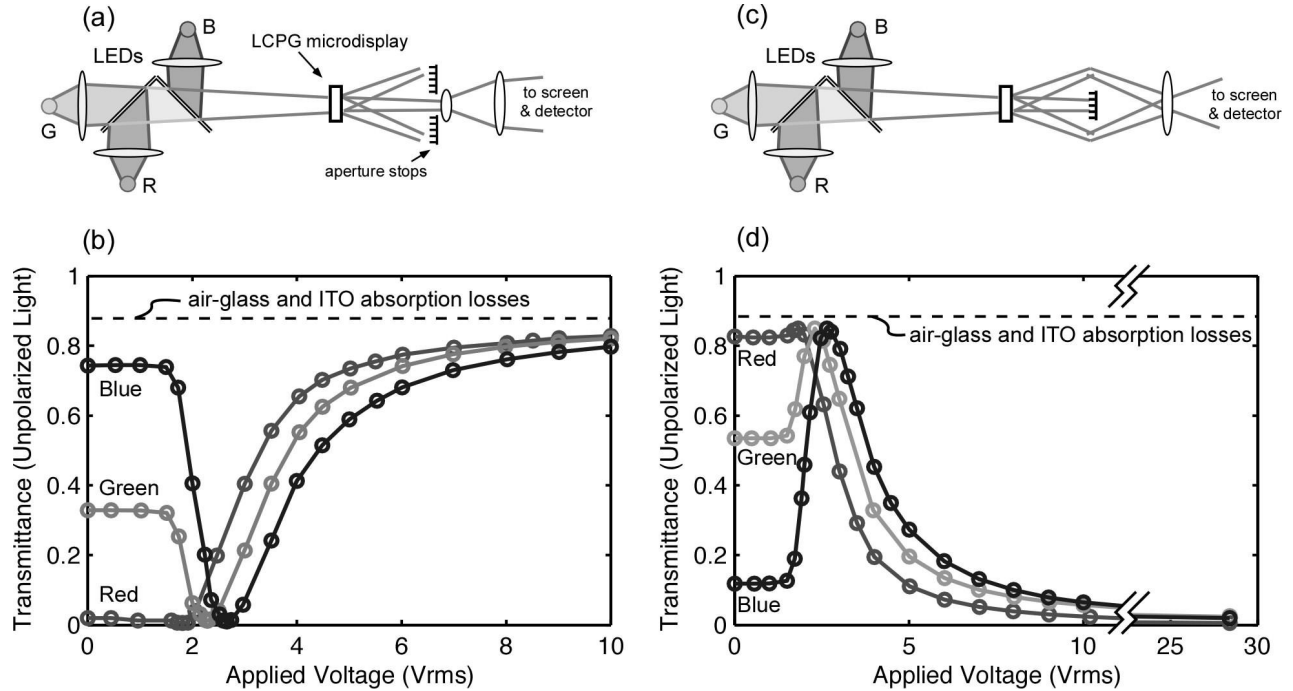


**Figure 5.** Modulation of unpolarized LED light by LCPG single pixel: (a) bright-field Schlieren projection scheme and (b) associated transmittance response to voltage; (c) dark-field Schlieren projection scheme and (d) associated transmittance response. In both cases, transmittance is calculated with respect to intensity when the LCPG and aperture-stop removed.

would offer the maximum possible contrast ratios for the LCPG modulator. We suspect the aperture-stop in our current implementation may be creating enough stray light leakage to affect the dark state, and we continue to investigate this. However, it should be clear that with further optimization that even higher contrast ratios could be in the dark-field configuration.

## 6. DISCUSSION

The LCPG structure experimentally demonstrated here is an attractive element for applications in diffractive optics, wide-angle beam-steering, tunable filters, and even polarimetry. One of the most compelling applications in our opinion remains that of the LCPG element as a polarization-independent microdisplay, uniquely enabling highly portable projection displays. However, in order to achieve systems based on this type of microdisplay that are competitive with current devices, we must consider its étendue (a geometric measure of the capacity to transmit light).

While a full analysis of the étendue for an LCPG microdisplay is beyond our present scope, we can make an estimate in simple terms. Consider Fig. 6(a), where diverging light is passing through the LCPG and is diffracted entirely into the 0- and  $\pm 1$ -orders. For high brightness and high contrast, no overlap in the solid angles formed by the diffraction order should occur. This requires that  $\theta_{diff} > 2\Omega$ , where  $\theta_{diff} = \sin^{-1}(\lambda_{Blue}/\Lambda)$  is the diffraction angle and  $\Omega$  is the half-angle of divergence of the light in the horizontal direction. Since shorter wavelengths diffract the least, we consider  $\lambda_{Blue}$  as the limiting case. The étendue of a rectangular microdisplay<sup>23</sup> can be expressed as:

$$E = 4A \sin \Omega \sin \Phi, \quad (4)$$

where  $A = (length)(width)$  is the total area of the modulator. A rough estimate of the projection lens  $f/\#$  matched to this SLM can be found by  $f/\# = \sqrt{\pi A_o/4E}$ , where  $A_o$  is the area of the lens that completely includes the SLM.

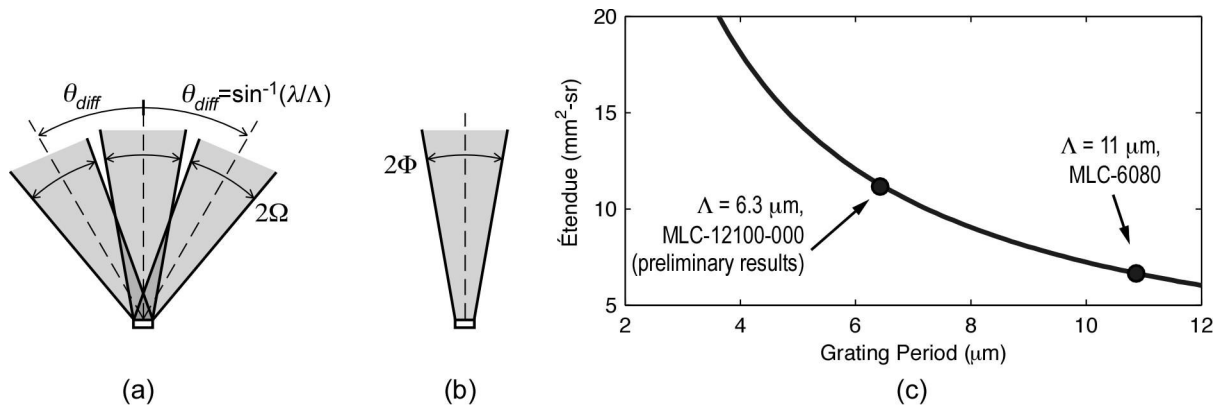


**Figure 6.** Estimating étendue for the LCPG spatial-light-modulator: (a) horizontal view showing diffraction of diverging light into only the 0- and  $\pm 1$ -orders, leading to the constraint  $\theta_{diff} > 2\Omega$ ; (b) vertical view; and (c) estimates of étendue of our experimental LCPG single-pixels (with active area  $(15\text{mm})^2$ ).

For the LCPG with  $\Lambda = 11\mu\text{m}$  discussed until now, the étendue was  $E = 6.6\text{mm}^2 - \text{sr}$ , where the size of the active area of the LCPG element was  $15 \times 15\text{mm}^2$ . The corresponding  $f/\# = 6.5$ , where in both estimates we have assumed a typical value of  $\Phi = 20^\circ$  for the vertical divergence half-angle of the incident light, which also corresponds to the value in our proof-of-concept platform in Fig. 5. In a recent development with a different LC material (MLC-12100-000, Merck,  $\Delta n = 0.113$ ), we have achieved a smaller grating period  $\Lambda = 6.3\mu\text{m}$  with  $d = 2.9\mu\text{m}$ . In this case improved values were achieved:  $E = 11.5\text{mm}^2 - \text{sr}$  and  $f/\# = 4.9$ . However, as calculated in Fig. 6(c), substantially smaller grating periods of  $\leq 3\mu\text{m}$  are needed to approach the étendue values of modern microdisplays.

## 7. CONCLUSIONS

We have experimentally demonstrated a liquid crystal diffraction grating with truly ideal properties, including  $\sim 100\%$  diffraction efficiencies and high contrast (600:1) for monochromatic light. We also show polarization-independent switching of LED light with promising contrast at modest drive voltages using the LCPG at grating periods of  $11\mu\text{m}$ . Surprisingly fast switching times of  $\leq 2\text{ms}$  are observed with nematic LCs. Very low scattering ( $< 0.3\%$ ) is observed throughout, and almost all diffracted light ( $\sim 99\%$ ) appears in the 0th- and 1st-orders. Smaller periods are desired in order to achieve high projection system performance, particularly to improve the étendue of SLMs based on the LCPG. We are persuaded that the LCPG shows great promise as the active element for compact, ultra-portable projection displays and other SLM applications.

## ACKNOWLEDGMENTS

The authors gratefully acknowledge the support of the National Science Foundation through a STTR Phase I grant (OII 0539552), in partnership with Southeast TechInventures Inc. and ImagineOptix Corp. MJE also thanks Dick Broer, Cees Bastiaansen, Carlos Sanchez, Jason Kekas, and Chongchang Mao for many fruitful technical discussions supporting this research.

## REFERENCES

1. M. J. Escuti and W. M. Jones, "Polarization independent switching with high contrast from a liquid crystal polarization grating," *SID Symposium Digest* **37**, pp. 1443–1446, 2006.
2. J. Chen, P. J. Bos, H. Vithana, and D. L. Johnson, "An electro-optically controlled liquid crystal diffraction grating," *Applied Physics Letters* **67**(18), pp. 2588–2590, 1995.
3. M. Honma, K. Yamamoto, and T. Nose, "Periodic reverse-twist nematic domains obtained by microrubbing patterns," *Journal of Applied Physics* **96**(10), pp. 5415–5419, 2004.

4. C. M. Titus and P. J. Bos, "Efficient, polarization-independent, reflective liquid crystal phase grating," *Applied Physics Letters* **71**(16), pp. 2239–2241, 1997.
5. B. Wang, X. Wang, and P. J. Bos, "Finite-difference time-domain calculations of a liquid-crystal-based switchable bragg grating," *journal of the Optical Society of America A* **21**(6), pp. 1066–1072, 2004.
6. B. Wen, G. Rolfe, and C. Rosenblatt, "Nematic liquid-crystal polarization gratings by modification of surface alignment," *Applied Optics* **41**, pp. 1246–1250, 2002.
7. Y. Zhang, B. Wang, D. B. Chung, J. Colegrove, and P. J. Bos, "Reflective polarization independent lc phase modulator with polymer wall," *SID Digest* **36**, pp. 1178–1181, 2005.
8. J. Eakin, Y. Xie, R. Pelcovits, M. D. Radcliffe, and G. Crawford, "Zero voltage freedericksz transition in periodically aligned liquid crystals," *Applied Physics Letters* **85**(10), pp. 1671–1673, 2004.
9. H. Sarkissian, J. B. Park, B. Y. Zeldovich, and N. V. Tabirian, "Potential application of periodically aligned liquid crystal cell for projection displays," *Proc. of CLEO/QELS Baltimore MD*, p. poster JThE12, 2005.
10. J. Tervo, V. Kettunen, M. Honkanen, and J. Turunen, "Design of space-variant diffractive polarization elements," *journal of the Optical Society of America A* **20**(2), pp. 282–289, 2003.
11. L. Nikolova and T. Todorov, "Diffraction efficiency and selectivity of polarization holographic recording," *Optica Acta* **31**, pp. 579–588, 1984.
12. J. Tervo and J. Turunen, "Paraxial-domain diffractive elements with 100% efficiency based on polarization gratings," *Optics Letters* **25**(11), pp. 785–786, 2000.
13. H. Sarkissian, S. V. Serak, N. Tabirian, L. B. Glebov, V. Rotar, and B. Y. Zeldovich, "Polarization-controlled switching between diffraction orders in transverse-periodically aligned nematic liquid crystals," *Optics Letters* **2006**(15), pp. 2248–2250, 2006.
14. S. Kakichashvili, "Polarizational (anisotropic-vectorial) holographic recording on practical photoanisotropic materials," *Opt. Spectrosc.* **42**, pp. 218–220, 1977.
15. P. Collings and M. Hird, *Introduction to Liquid Crystals*, Taylor and Francis Ltd, London, 1998. whole book.
16. P. Rudquist, L. Komitov, and S. T. Lagerwall, "Linear electro-optic effect in a cholesteric liquid crystal," *Physical Review E* **50**(6), pp. 4735–4743, 1994.
17. X. Wang and J. Yao, "Transmitted and tuning characteristics of birefringent filters," *Applied Optics* **31**(22), pp. 4505–4508, 1992.
18. G. Crawford, J. Eakin, M. D. Radcliffe, A. Callan-Jones, and R. Pelcovits, "Liquid-crystal diffraction gratings using polarization holography alignment techniques," *journal of Applied Physics* **98**, p. 123102, 2005.
19. M. Schadt, H. Seiberle, and A. Schuster, "Optical patterning of multi-domain liquid-crystal displays with wide viewing angles," *Nature* **381**, pp. 212–215, 1996.
20. C. Oh, R. Komanduri, and M. J. Escuti, "FDTD and elastic continuum analysis of the liquid crystal polarization grating," *SID Symposium Digest* **37**, pp. 844–847, 2006.
21. P. Yeh and C. Gu, *Optics of Liquid Crystal Displays*, John Wiley and Sons, Inc., New York, 1999.
22. W. M. Jones, B. L. Conover, and M. J. Escuti, "Evaluation of projection schemes for the liquid crystal polarization grating operating on unpolarized light," *SID Symposium Digest* **37**, pp. 1015–1018, 2006.
23. E. H. Stupp and M. S. Brennessoltz, *Projection Displays*, John Wiley and Sons Ltd., New York, 1999.